Green Analytical Chemistry 19 (2026) 100385

Contents lists available at ScienceDirect

Green Analytical Chemistry

journal homepage: www.elsevier.com/locate/greeac

Automated derivatization and sample preparation protocol for ultrashort-chain PFCAs of water samples for GC-MS/MS detection

Rouven Häusler [a,*], Alexander Laver [a], Johanna Freilinger [b,d], Hagen M. Gegner [c], Marco Rupprich [d], Daniel Häussinger [e], Stefan Gaugler [a]

[a] Institute for Chemistry and Bioanalytics, University of Applied Sciences Northwestern Switzerland, Hofackerstrasse 30, 4132 Muttenz, Switzerland
[b] Institute of Analytical Chemistry and Radiochemistry, Leopold-Franzens-University Innsbruck, Austria
[c] CTC Analytics AG, Industriestrasse 20, 4222 Zwingen, Switzerland
[d] Institute for Ecopreneurship, University of Applied Sciences Northwestern Switzerland, Hofackerstrasse 30, 4132 Muttenz, Switzerland
[e] Department of Chemistry, University of Basel, St. Johanns-Ring 19, 4056 Basel, Switzerland

ARTICLE INFO

Keywords:
PFCAs, GC-MS
Derivatization, automation
Environmental analysis

ABSTRACT

This study presents a robust and largely automated workflow for the determination of ultra short-chain perfluorocarboxylic acids (PFCAs) in water by GC–MS/MS following in-vial derivatization with diphenyl diazomethane (DDM). The method combines two robotic platforms: one performs automated synthesis, cooling and dispensing of the DDM reagent, while the other carries out µSPE enrichment of water samples. Using the high resolution of gas chromatography with pulsed splitless injection provided low-noise baselines, well-defined peak shapes and highly reproducible automated integration. Method validation showed acceptable recoveries and precision according to the ICH guideline over a concentration range from 0.1 – 50 µg/L. Detection limits range from 0.26 – 0.52 pg on column and although they do not surpass the most sensitive LC-MS/MS methods, they are fit-for-purpose in an established workflow optimized for robustness, effectiveness and sustainability. Comparison of micro solid phase extraction (µSPE) cartridge loading by syringe driver (SD) versus the robotic system demonstrated similar retention performance but substantially reduced hands-on time and more standardized operation mode with the automated robotic system. The µSPE cartridges drastically lower the use of sorbent material by 90% and polypropylene housing by 75% compared to conventional applied SPE materials. The fully automated protocol consumes <1 mL of methanol per sample, achieving a > 95% reduction in organic solvent consumption relative to standard protocols. Application to Swiss tap, filter and surface waters revealed ubiquitous occurrence of trifluoroacetic acid, underscoring the need to monitor ultra short-chain PFCAs in the environment.

1. Introduction

Per- and polyfluoroalkyl substances (PFAS) have gained increasing interest over the past few decades [1]. By definition of the Organization for Economic Co-operation and Development (OECD), a compound requires at least one fully fluorinated methyl (–CF_3) or methylene (–CF_2–) group to be classified as PFAS [2]. This broad definition includes millions of molecules that can be referred to as PFAS [3]. The database of PubChem, for example, contains around seven million compounds that match this description. On an industrial and commercial level, however, only a few thousand PFAS are relevant [4]. They are used in many applications and processes, such as water- and greaseproof surfaces in food packaging, textiles or cookware, aqueous film forming foam or friction-reducing wax. Their unique properties make it very challenging to find any substitute materials to replace them in various fields of application [5].

Certain PFAS have already been linked to human health risks. Chemical manufacturers of PFAS at the time began conducting health risk studies in the 1960s. Over the decades, the data showed troublesome contamination of workplaces and the environment. Despite early indicators of non-negligible health risks, these findings were historically under-investigated and poorly communicated to the public. Although there is still debate and discussion on the toxicity, especially for the

* Corresponding author.
E-mail addresses: rouven.haeusler@fhnw.ch (R. Häusler), alexander.laver@fhnw.ch (A. Laver), johanna.freilinger@uibk.ac.at (J. Freilinger), hgegner@ctc.ch (H.M. Gegner), marco.rupprich@fhnw.ch (M. Rupprich), daniel.haeussinger@unibas.ch (D. Häussinger), stefan.gaugler@fhnw.ch (S. Gaugler).

https://doi.org/10.1016/j.greeac.2026.100385
Received 16 June 2026; Received in revised form 17 August 2026; Accepted 19 August 2026
Available online 26 August 2026

Abbreviations

PFAS	per- and polyfluoroalkyl substances
PFCA	perfluorocarboxylic acids
TFA	trifluoracetic acid
PFPrA	pentafluoropropionic acid
PFBA	heptafluorobutyric acid
DDM	diphenyl diazomethane
DCM	dichloromethane
EF	enrichment factor
PP	polypropylene
SPE	solid phase extraction
ISTD	internal standard
GC	gas chromatography
RPLC	reverse-phased liquid chromatography
MS	mass spectrometry
dMRM	dynamic multiple reaction monitoring
SD	syringe driver
EI	electron ionization
HS	headspace
RTC	robotic tool change

different kinds of PFAS, increasing evidence has been found to underline these concerns [6]. Most recent studies assessed damaging effects on the liver, interference with the endocrine system, suppression of the immune response, and carcinogenicity. However, the full extent is still unresolved [5,7]. Faced with these alarming facts, the European Commission stated for the first time in 2010 that all member states were obliged to monitor the presence of PFAS in food products [8]. In 2020, the use of certain PFAS in food contact material was restricted by the European Union (EU). Some member states intended even more drastic measures, extending the ban to other industrial sectors [9]. Since 2020, the EU law states a threshold limit of <500 ng/L total PFAS and PFAS-20 (list of 20 PFAS) sum parameter of <100 ng/L for water intended for human consumption [10,11].

PFAS are often called "forever chemicals" [6,12]. The bond dissociation energy of the carbon-fluorine bond is 485 kJ/mol and thereby labeled as the strongest in organic chemistry [12]. They are highly persistent because of their resistance to oxidative and reductive degradation under environmental conditions [13]. Perfluorinated carboxylic acids (PFCAs) are among the most frequently detected PFAS in environmental matrices and therefore are of considerable relevance in environmental analytics [14]. Especially ultra-short-chain ($C < 4$) PFCAs have been detected in various matrices [15,16]. Owing to their short carbon backbone and the acidic functional group, these compounds are often predominantly present as negatively charged, highly water-soluble species at environmentally relevant pH values. Hence, their potential for bioaccumulation in humans is lower than that of short- ($4 \leq C \leq 8$) and long-chain ($C > 8$) PFCAs [17]. Nevertheless, the ubiquitous occurrence of trifluoroacetic acid (TFA) has raised considerable concern and is currently the subject of intensive investigation. Based on animal studies, the Risk Assessment Committee (RAC) of the European Chemicals Agency (ECHA) is currently considering the reclassification of TFA and its salts as reprotoxic 1B [18]. Taken together, their combination of apparent regulatory concern, increasing environmental burdens, and still incomplete toxicity data underlines the need to include ultra-short-chain PFCAs in environmental monitoring programs and future risk assessments [19].

Several non-specific methods are available to determine the total organic fluorine (TOF) in water samples such as combustion ionic chromatography (CIC) or ^{19}F nuclear magnetic resonance (NMR) spectroscopy [20]. While they give a more comprehensive picture of TOF, they are currently not reaching required sensitivity for direct analysis in water samples with low sample volumes [21]. The targeted determination of PFAS however, is usually performed by high-performance liquid chromatography (HPLC) or gas chromatography (GC) coupled with mass spectrometry (MS). HPLC-MS is the state of the art in analytical chemistry for the measurement of most ionic and long-chain PFAS [12]. GC–MS coupled with electron ionization (EI) is a suitable tool for the analysis of volatile and neutral PFAS [22]. This also includes ultrashort-chain PFCAs, which are often derivatized for enhanced analytical performance. However, these approaches subject the derivatives to a higher risk of degradation for example by moisture [23]. In this study, we developed an analytical method which is precedented by an automated *in-situ* derivatization of preconcentrated water samples. The presented derivatization procedure aims for robust analytics and high sample throughput while minimizing environmental and laboratory contamination that could lead to false positives.

We thereby overcome typical problems of retention time issues for polar, early eluting compounds in classical reverse-phased LC (RPLC), such as peak broadening, elevated background level and ion suppression due to matrix components.

2. Materials and methodology

2.1. Reagents

Trifluoroacetic acid (TFA, >99%), Pentafluoropropionic acid (PFPrA, >97%) and Heptafluorobutyric acid (PFBA, >98%) were purchased from Merck. The internal standard (ISTD) sodium trifluoroacetate-$^{13}C_2$ was acquired from Toronto research chemicals (1 mg, PFCA-^{13}C-ISTD, >98%) and perfluoro-*n*-($^{13}C_4$) butanoic acid (50 µg/mL in methanol; PFCA-^{13}C-ISTD, >99%) from Wellington Laboratories. Formic acid (>99%), HPLC-grade ethyl acetate and methanol were obtained from Thermo Fisher. An in-house Agilent Milli-Q water dispenser (>18 MΩ·cm) was used in this study.

For the synthesis of the derivatization reagent, dichloromethane (DCM), anhydrous magnesium sulfate ($MgSO_4$), benzophenone hydrazone (>98%) and activated manganese dioxide were purchased from Merck.

2.2. Analytical instrument and method

The GC–MS system consisted of an Agilent 8890 GC system coupled with an Agilent 7010D GC/TQ mass analyzer with a high efficiency source (HES) 2.0 source. Two 15 m × 0.25 mm × 0.25 µm DB-5 MS UI GC-columns were serially connected for compound separation. This configuration was chosen to simplify maintenance and to minimize the risk of contamination from incomplete backflushing of the entire column.

Pure helium (CarbaGas, Switzerland, 99.9999%) was used a carrier gas with a flow rate of 1 mL/min and N_2 as collision gas in dynamic multiple reaction monitoring (dMRM) operation mode. The inlet liner (single taper Ultra Inert, 4 mm ID, 900 µL) was heated to 240 °C and pulsed (25 psi) splitless injection was used. The GC–MS was mounted with a Gerstel MultiPurposeSampler (MPS) Robotic Dual Head autosampler (Gerstel, Mülheim, Germany) which was equipped with a 10 µL syringe to perform injections of 1 µL sample volume.

The oven temperature program starting at 80 °C was ramped at 25 °C/min to 130 °C (0.5 min hold), followed by a ramp of 15 °C/min to 190 °C (1.0 min hold) and a final ramp of 30 °C/min to 265 °C (1.0 min hold). After each run, a 2 min post-run at 300 °C with a 2 mL/min backflush was applied to remove nonvolatile matrix components and excess DDM byproducts, protecting the analytical column and MS source. Including the analytical run (11 min), the 2 min post-run and a 2 min oven equilibration period, the GC cycle time per injection was 15 min, corresponding to the total time required for the system to return to a ready state for the next sample.

2.3. SPE and sample preparation

Surface water from different sources, tap, fountain water and filter effluents of charcoal-treated water at drinking water production sites were collected in 50 mL Falcon tubes. All the samples were supplied by the authors and originated invariably from Switzerland. After centrifugation at 5000 rpm for 20 min, the supernatant was transferred and spiked with 5 µg/L of both ISTDs for further processing.

Micro solid phase extraction (µSPE) was performed on an automated PAL robotic tool change (RTC) automated sample preparation system (CTC Analytics, Zwingen, Switzerland). This system is hereafter referred to as PAL µSPE RTC. As a sorbent material, a PFAS selective polymer with a dual binding mechanism published and supplied by Freilinger *et al.* was used. This highly crosslinked reusable material uses 3-(1H,1H,2H,2H-perfluorooctyl)-1-vinylimidazolium chlorid therefore providing fluorophilic as well as electrostatic binding sites. They have already demonstrated excellent selective retention for a list of PFAS from different water matrices along with high total loading capacities with a sharp breakthrough curve [24]. Commercial alternative sorbents have often demonstrated fluctuating and low recoveries (<50%) for ultrashort-chain PFCAs in matrix-loaded water samples [25–27]. The µSPE cartridges were prepared containing 20 mg of sorbent packed between two filters. The finely ground polymer was weighed in on a XPR226DR analytical balance (Mettler TOLEDO, Greifensee, Switzerland) with an automated powder dosing head. An in-house mechanical press was employed to control and standardize the compression force applied to the µSPE cartridges. The composition is described in detail in Fig. 1.

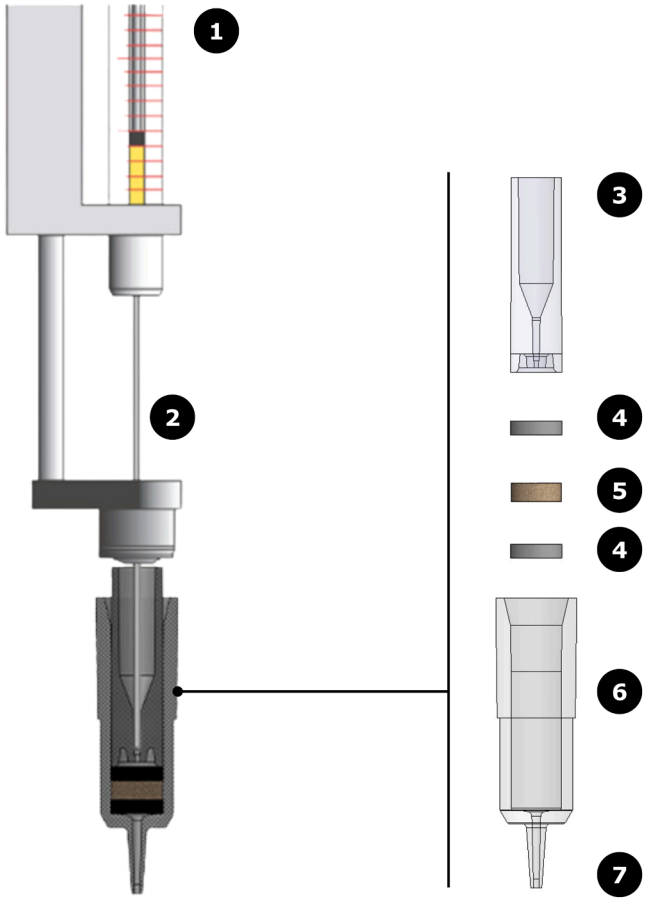

Fig. 1. Composition of the µSPE cartridge and application mode using an autosampler smart syringe; 1 = syringe body, 2 = syringe needle, 3 = inner body (PP), 4 = filter disks (HDPE), 5 = PFAS selective sorbent material, 6 = outer body (PP), 7 = cartridge outlet for direct elution into a vial.

The PAL robot conditioned the µSPE cartridges with 200 µL of each methanol and Milli-Q water in sequence. The 1 mL smart syringe worked as solvent pump with a constant flow and pressure. The samples were placed on the PAL robot in 10 mL glass headspace (HS) vials. After loading the cartridges, they were washed with 120 µL MeOH:Milli-Q water 1:9 and eluted with 300 µL of a methanolic solution containing each 0.5% w/w LiCl and NH_4Cl, 0.5 vol-% formic acid into a 2 mL analytical vial.

For larger sample amounts and process parallelization, a syringe driver (Niscomed, Delhi, India) was tested with polypropylene (PP) syringes with volumes up to 50 mL. They were manually loaded and a preconditioned µSPE cartridge was fitted tightly on top. After loading onto the cartridge, it was then further automatically processed on the PAL µSPE RTC.

In a last step, the analytical vials containing 300 µL eluate were dried in an Genevac EZ-2 Elite centrifugal evaporator (SP Industries, Ipswich, United Kingdom) for 20 min and immediately resuspended in 290 µL ethyl acetate and 10 µL derivatization solution just before analysis. With loss of nitrogen (N_2), DDM reacts with PFCA to the corresponding diphenyl methyl ester [28]. After 1 min of agitation with 400 rpm at ambient conditions, they were subjected to GC–MS/MS analysis.

2.4. Synthesis protocol for DDM

The synthesis procedure was adapted from a study published in continuous flow chemistry [29]. The hydrazone was oxidized to the corresponding diazo compound using activated MnO_2 (Scheme 1). A preliminary laboratory experiment was conducted to evaluate the efficiency and feasibility of the reaction process. Educt conversion was later characterized by ^{1}H-NMR spectroscopy. The following workflow was established on another PAL RTC, which is hereafter referred to by this designation.

Anhydrous $MgSO_4$ (66 mg, 1.0 eq.) and activated MnO_2 (175 mg, 4.0 eq.) were added together with dichloromethane (DCM, 0.8 mL) in a 2 mL brown glass vial. The vial was cooled to 4 °C in a Peltier stack refrigerating drawer for 30 min on the PAL robot. Benzophenone hydrazone (100 mg, 1.0 eq.) dissolved in DCM (0.6 mL) was added with a 1 mL autosampler smart syringe to the precooled solution.

A repeating cycle of cooling (4 °C) and vortex agitation at room temperature was performed on the PAL RTC. Vial transfers were performed using a magnetic robotic needle guide, which engages with magnetic vial caps to enable automated handling. The solution was vortexed on a vortex mixer module for 30 s at 300 rpm and then stored in the refrigerating drawer for 30 s. The total vortex time added up to 2 h, corresponding to 240 cycles. The vial with the deep red solution was centrifuged on a PAL centrifuge module. In a last step, dilutions were prepared by the PAL RTC to prefilled brown 2 mL vials containing DCM, yielding 0.1 M DDM solutions ready for use.

3. Results and discussion

3.1. DDM synthesis

In-process controls to monitor the synthesis of DDM were measured with time-resolved ^{1}H-NMR spectroscopy in $CDCl_3$ (Fig. S2 - S5). After 5 min, the educt-to-product ratio was approximately 1:1, indicating rapid initial conversion. The ratio was calculated comparing equivalent, non-overlapping signals from DDM at δ 7.19 ppm and benzophenone hydrazone at δ 7.53 ppm. After 1 h, the residual starting-material signal intensity had decreased to approximately one quarter of the product signal, and after 2 h less than 5% of benzophenone hydrazone remained. One hour later, there was still the same amount of educt, but new aromatic proton signals started to appear in the range of δ 7.2 – 7.4 ppm, partially overlapping with the aromatic signals of DDM. On this basis, a reaction time of 2 h was defined as the optimal compromise between educt depletion and by-product formation. Additionally, trace amounts

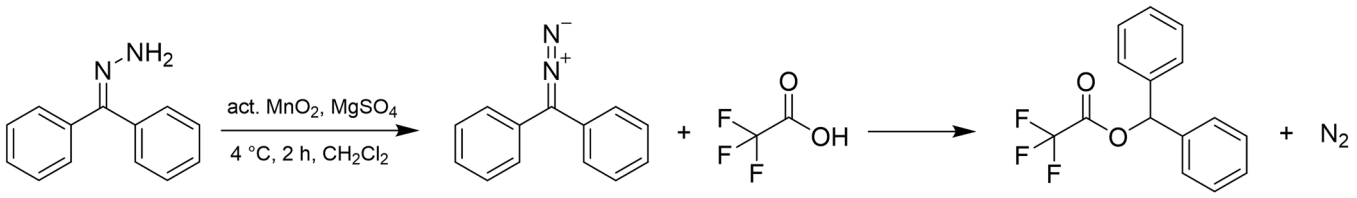

Scheme 1. Automated synthesis of DDM and derivatization reaction at the example of TFA.

of benzophenone (most low-field shifted aromatic signal at δ 7.8 ppm [35]) were consistently detected in all in-process control samples, but did not increase significantly over the course of the experiment. The resulting DDM solution was of sufficient purity to ensure efficient derivatization of PFCAs while keeping the level of side products to a minimum.

3.2. Evaporation and derivatization procedure

Evaporation of samples in the centrifugal evaporator could be processed simultaneously in batches of up to 54 vials. Blind samples containing pure eluent were placed next to QC samples, but no significant cross-contamination was detected (< blank offset). The loss of volatile ultrashort-chain PFCAs was countered by the salt formation to the corresponding acetate with the available lithium and ammonium salts, thereby increasing the analytes boiling point. Ethyl acetate and DCM proved to dissolve the PFCAs, but the salt rested as precipitate on the vial bottom. No notable time dependence of the derivatization in the vial was observed; signal intensity remained essentially constant when the derivatizing agent was added and the mixture was agitated for more than 10 min.

Silylation and esterification protocols for short- and ultra-short chain PFCAs generally required prolonged reaction times at elevated temperatures or the use of relatively hazardous reagents and catalysts such as H_2SO_4 or diazomethane [36,37]. In contrast, DDM provides the simplest reaction profile, eliminating the need for heating and extended incubations that are typical of conventional silylation and esterification approaches while also covering long-chain PFCAs [28].

3.3. Cartridge loading

The loading of the sample on µSPE cartridges was tested with a SD and compared to the PAL µSPE RTC. A prefilled PP-syringe was equipped with a µSPE cartridge on top by simply clamping it on the syringe outlet. There was no case where the backpressure would cause detachment of the cartridge. The syringe dispense speed was set to 10 µL/s in accordance with the PAL µSPE workflow. Cartridge elution was performed on the PAL µSPE RTC, yielding 300 µL of concentrated eluate.

The sample processing on the PAL µSPE RTC proceeded in a combined method of cartridge preconditioning, sample loading and elution. This decreased manual effort, as entire sequences were processed autonomously. A maximum sample volume of 8 mL could reproducibly be extracted from the 10 mL HS vial. Otherwise, the smart syringe was prone to pull up air together with the sample liquid as the bottom of the vial was not fully reached. For higher sample loading, the volume was split up into different 10 mL HS vial.

The analytical performance of syringe-driven and PAL-based µSPE cartridge loading was compared at two spike levels with final concentrations of 10 and 100 µg/L in the eluate. Milli-Q water sample volumes in the range of 1 – 50 mL were tested for both applications (see Fig. 2).

Syringe-driven and PAL-based µSPE systems showed mean recoveries of 80% to 120% and associated RSDs (<20%) for all analytes, except for two outliers with 1 mL sample load at the lower concentration level.

Overall, the experiment demonstrated that both approaches estimate the true concentration with an accuracy of ±12% for loading volumes of

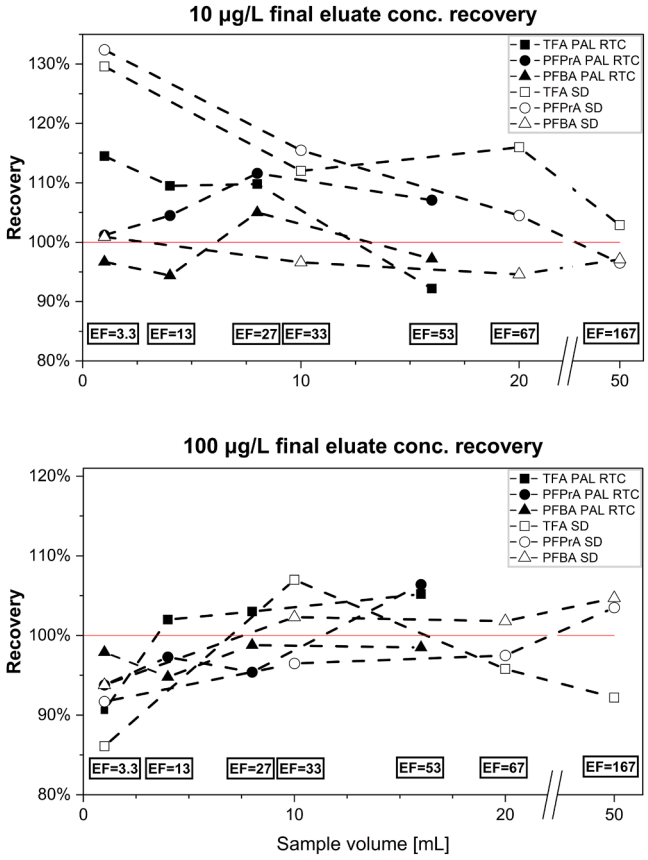

Fig. 2. Recoveries for Milli-Q water spiked to yield final eluate concentrations of 10 and 100 µg/L. Applied sample volumes ranged from 1 - 50 mL on the syringe driver (SD) and 1 to 16 mL on the PAL µSPE RTC. Rounded theoretical enrichment factors (EF; a relative metric for analyte enrichment) are reported for each sample volume and arise from the varying sample loading volumes. The initial concentrations in the spiked Milli-Q water differ accordingly.

≥8 mL. Neither significant breakthrough nor unusual retention was observed. This also proved that the solvent exchange from salty, acidified methanol to ethyl acetate and DDM solution yielded viable results.

At the 1 mL sample volume, individual recovery values for TFA and PFPrA on the SD were elevated, at approximately 130%. At the same time, such low volumes are atypical in sample preparation for trace analysis, as the enrichment factor (EF) is low, 3.3 in this case. In general, recoveries of all analytes improved with higher sample volume. This is coherent, as small volumes with a high concentration are more sensitive to deviation in the sample preparation step. Although there was no evidence of inferior analytical performance for enrichment with the SD, the manual syringe handling was more time consuming and is susceptible to variability depending on the operator, thus diminishing the reproducibility. The PAL robot followed a standardized protocol that was independent of the operator. Cartridge loading required more time, as the sample was processed in sequential 1 mL increments.

In contrast, the PAL workflow required no further hands-on time

once the samples were positioned. The sequence was run overnight and the eluted samples were collected from the rack the next day. The SD handling involved the preparation of the syringe and the transfer of the cartridge to the PAL robot for elution.

Use of consumable was relatively low for both systems; per sample, either a single PP syringe or one 10 mL glass headspace vial was required. The µSPE cartridge is made of ultra-pure PP with an average mass of 1.02 g and contains 20 mg of sorbent. Compared with conventional 6 cc Oasis WAX/GCB cartridges (~4 g PP and typically 200 mg sorbent), this corresponds to 75% reduction in plastics and 90% in sorbent material for single use of the cartridge. Methanol consumption was likewise downscaled to 860 µL per sample, including cartridge reconditioning, of which 560 µL was used for sample concentration and elution. In EPA Method 1633, at least 22 mL of methanol are used for the full SPE workflow of aquatic samples. In contrast, the developed protocol achieves a reduction in methanol consumption of >95% per worked-up sample. Also, N_2-evaporation for increasing the concentration after sample elution was avoided, a step frequently employed in conventional analytical workflows. This prevents the volatilization and release of organic solvents into the laboratory environment, thereby reducing the occupational exposure. This represents a significant advantage from both a safety and sustainability perspective, particularly in routine high-throughput analytical workflows.

The µSPE cartridge was reusable upon rinsing it with the acidified, salty methanolic solution and further reconditioning with methanol and Milli-Q water. However, in this study, none of the cartridges were used twice, further studies to test the feasibility are necessary. So far, Freilinger *et al.* proved stable recoveries (RSD <6%) for PFBA and three more PFAS from aqueous matrices [24].

3.4. Analytical method

The GC–MS/MS method was optimized to provide robust separation and sensitive detection of the derivatized PFCAs while maintaining a total run time compatible with routine analysis. TFA and PFPrA could not be chromatographically resolved and co-eluted, but they were reliably distinguished by their specific MRM's visible in Fig. 3. This made quantification of both analytes viable using the $^{13}C_2$-labled TFA. The oven temperature program was adjusted to provide a compromise between resolution, peak shape and throughput. For each compound, one quantifier and qualifier mass transition were recorded. A comprehensive summary of all MS/MS acquisition parameters is provided in Table 1.

Derivatization shifted the precursor→product ion transitions to higher *m/z* values compared with the underivatized analytes. Diphenyl methane increases the offset for each derivatized precursor ion by 166 *m/z* units. Monitoring ions with higher *m/z* often reduces the background noise and isobaric interferences, improving the specificity for assignment of the target analytes [30].

The selected transitions produced well-resolved, symmetric chromatographic peaks with low-noise baselines with minimal fluctuations, as suggested by the S/N ratios at the lowest calibration level in Table 1. Retention times for all target analytes were highly repeatable across batches with deviations <0.02 min from the reference chromatogram. The indicated retention times, analyte/ISTD ratios and automated integration remained consistent over several batches.

In the validation phase, a calibration function was recorded to perform statistical analysis. The neat calibration ranged from 0.1 – 50

Table 1
Validated MS/MS method parameters. Absolute retention time shifts were evaluated across all nine calibration level samples.

Analyte	Retention time [min]	LOD / LOQ [pg on column/ µg/L in sample]	Mass fragment transition [*m/z*]	Collison energy [V]	S/N at lowest calibration level
TFA	6.55 ± 0.01	0.52 / 1.59	280 → 166 (quant)	10	68
			280 → 279 (qual)	8	33
PFPrA	6.57 ± 0.01	0.44 / 1.33	330 → 166 (quant)	10	54
			330 → 329 (qual)	8	4
PFBA	6.88 ± 0.01	0.26 / 0.81	380 → 166 (quant)	9	76
			380 → 379 (qual)	6	21

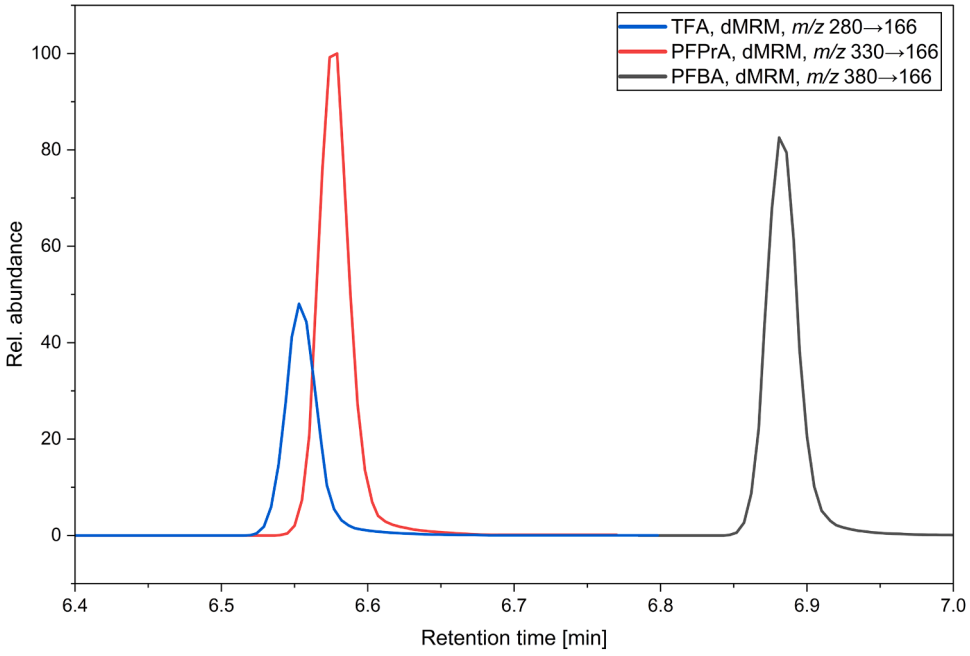

Fig. 3. Chromatogram of the quantifier dMRM transitions indicated in the top right box.

µg/L with 9 levels and R^2 >0.99. While the calculated RSD of reproducibility samples was <20% at the calibration levels of 5 µg/L and 25 µg/L with n = 6. Spike-recovery experiments yielded recoveries between 80% and 120%. System blanks were consistently below the lower limit of the calibration. However, as all calibration levels showed a measurable TFA response of >0.1 to <0.25 µg/L attributed to ethyl acetate, ISTDs and DDM solution. Consequently, the calibration curve in this and subsequent sequences was fitted with a non-zero blank offset to correct for this contribution.

The limit of quantification (LOQ) and limit of detection (LOD) were calculated following the ICH guideline [31]. Regression analysis provided the residual sum of squares (RSS), by which the standard deviation of the y-intercept was calculated. For the LOD, this value was multiplied by 3.3 respectively 10 for the LOQ and divided by the slope of the curve.

A fundamental issue was the close gap between TFA and its $^{13}C_2$-labeled ISTD of M + 2. This made a narrow MRM mass window essential to minimize signal overlap with the DDM-derivatized TFA. The 13 carbon atoms of diphenyl methyl give a raise to the M + 1 fragment of ~14%. At low concentration levels, this effect is less severe, but it certainly contributed to the higher deviations in analyte/ISTD ratios of TFA and PFPrA compared to PFBA, leading to an accordingly elevated LOQ of the analytical method.

The selected calibration reflects the fact that the workflow relies on preconcentration of water samples prior to instrumental analysis and is aligned with native TFA concentrations reported by Henne *et al.*, who found levels of approximately 0.33 – 0.88 µg/L in Swiss rivers [32].

Reported LODs for recent LC-MS/MS and IC-MS/MS methods are spread over a broad range. For TFA in water samples, performance of LC-MS/MS methods are ranged from 3 – 187 ng/L respectively 0.09 – 27 ng/L for IC-MS/MS [33]. Thus, these systems achieve lower nominal detection limits than the presented method. However, LC-MS/MS and IC-MS/MS are often practically constrained by ubiquitous TFA background in solvents, laboratory water and LC systems, so effective quantification limits are determined by blank contamination rather than instrumental sensitivity [34]. In contrast, the automated workflow employs just-in-time derivatization and avoids routine use of TFA within the chromatographic system, thereby minimizing on-system contamination and enhancing signal quality and resolution.

3.5. Water sample analysis

The water samples were measured with the dual PAL robot work-up. Single measurements of the samples were executed. Quality control standards after ten measurements guaranteed the instrument method reliability. Ultimately, TFA was conclusively detected in each sample. Concentrations of PFPrA and PFBA were in some cases still not quantifiable with a 27-fold enrichment as indicated in Table 2. Complying with the method detection limits, the detectable concentrations were around 16.7 ng/L for PFPrA and 10 ng/L for PFBA.

Tap water TFA concentrations ranged from 94.1 ng/L to 248 ng/L, corresponding to a 2.6-fold variation between the minimal and maximum values (see Fig. 4). In contrast, unrelated surface water samples from rivers, ponds and lakes resulted in a mean value of 132 ng/L with double the sample size. This was found to be lower compared to tap water (174 ng/L), which suggests that other subsurface sources lead to a progressive enrichment of TFA in the water destined for drinking-water production of the here investigated samples.

Fountain water samples were collected from the same site in a single week once per day. With a mean value close to 58 ng/L and a very low RSD of around 3.5%, a coherent result was found for both the method as well as the steady concentration in the fountain water.

No statistical analysis was possible with the three filter effluents. However, they perfectly illustrated that the most commonly used active charcoal filter failed to retain TFA and the other two PFCAs from the panel. The abundance in natural water and the properties of these compounds pose a well-known problem for complete removal even in our drinking water.

Table 2
Overview of analysis results for PFPrA and PFBA in all tested water samples.

Analyte	Domain	N_{tot} samples	*N* samples > LOD	c_{max} measured [ng/L]
PFPrA	Tap water	10	8	46.7
	Surface water	20	14	39.2
	Fountain water	7	2	18.8
	Drinking water filter effluent	3	2	41.1
PFBA	Tap water	10	7	59.5
	Surface water	20	16	28.9
	Fountain water	7	7	17.2
	Drinking water filter effluent	3	2	187

4. Conclusion

The presented workflow demonstrated that analysis of ultrashort-chain PFCAs by GC–MS/MS can be built around robustness, effectiveness and sustainability rather than pushing absolute detection limits. Automated µSPE on PAL µSPE RTC platforms provide efficient enrichment with only a few hundred microliters of eluent, reducing solvent consumption and minimizing consumable waste compared with conventional SPE, while still achieving high concentration factors. In the dual PAL robot setup, water samples are enriched on cartridges by the PAL µSPE RTC while another PAL RTC synthesizes, cools and dispenses the DDM derivatization reagent, fully exploiting overlapping, time-consuming steps, to maintain high throughput. Robotic preparation and handling of the DDM solution reduces operator exposure and standardizes contact times and temperatures. *In-situ* derivatization of PFCAs with freshly synthesized DDM-solutions can be accordingly scheduled to guarantee real time, standardized analysis of the samples. Although the achieved detection limits of the MS method are not the lowest reported for PFCAs, they are adequate for environmental samples in combination with an SPE workflow that significantly reduces hands-on time compared to manual syringe-based loading while maintaining comparable total processing time. Further work is required to characterize the regeneration properties and limits of the µSPE cartridges in the developed setup. Systematic investigation of cartridge reconditioning conditions and permissible reuse cycles is warranted, as this would enable a more circulatory use of sorbent and solvent and further enhance the environmental sustainability of the workflow. Also, the lifetime of the GC column, especially long-term robustness of the peak shape and retention time, could be further determined for specific quality assessments. Overall, this dual-PAL, in-vial DDM derivatization approach exemplifies how automation can deliver reliable PFAS data with reduced labor, improved safety and better long-term sustainability of routine monitoring programs.

CRediT authorship contribution statement

Rouven Häusler: Writing – original draft, Validation, Investigation. **Alexander Laver:** Investigation. **Johanna Freilinger:** Writing – review & editing, Resources. **Hagen M. Gegner:** Writing – review & editing, Visualization. **Marco Rupprich:** Writing – review & editing, Resources. **Daniel Häussinger:** Writing – review & editing, Supervision. **Stefan Gaugler:** Writing – review & editing, Supervision, Resources, Funding acquisition.

Declaration of competing interest

The authors declare the following financial interests/personal relationships which may be considered; Johanna Freilinger and Marco Rupprich have patent #WO2025191130A1; EP4616941A1 pending to

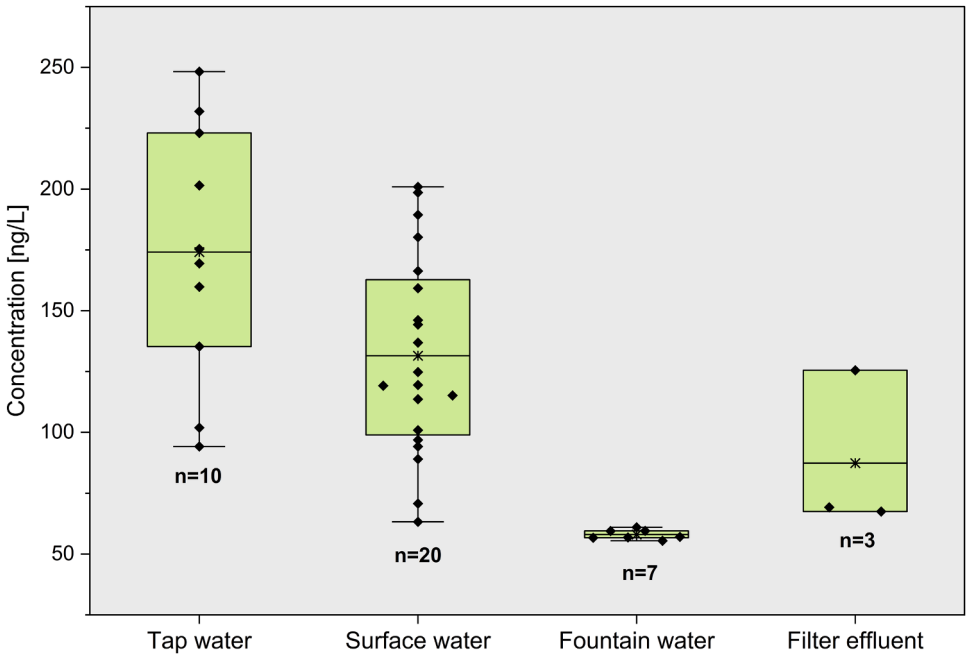

Fig. 4. Analysis results for TFA in all tested water samples. Displayed is the range of all measured values, the mean value and in the green box the range from lower and upper quartile.

AirPlus Ltd. Marco Rupprich reports a relationship with AirPlus Ltd. that includes equity or stocks.

Acknowledgments

The funding for this study was provided by Innosuisse – Swiss Innovation Agency, project "Fully automated comprehensive PFAS monitoring" (Project No. 124.619 IP-EE, 20.12.2024).

Supplementary materials

Supplementary material associated with this article can be found, in the online version, at doi:10.1016/j.greeac.2026.100385.

Data availability

Data will be made available on request.

References

[1] K.E. Pelch, A. Reade, C.F. Kwiatkowski, et al., The PFAS-Tox Database: a systematic evidence map of health studies on 29 per- and polyfluoroalkyl substances, Env. Int. 167 (2022) 107408, https://doi.org/10.1016/j.envint.2022.107408.
[2] OECD, Reconciling Terminology of the Universe of Per- and Polyfluoroalkyl Substances: recommendations and Practical Guidance, Recommendations and Practical Guide, OECD Ser. Risk Manag. (61) (2021).
[3] R.C. Buck, J. Franklin, U. Berger, et al., Perfluoroalkyl and polyfluoroalkyl substances in the environment: terminology, classification, and origins, Integr. Env. Assess. Manag. 7 (2011) 513–541, https://doi.org/10.1002/ieam.258.
[4] E.L. Schymanski, J. Zhang, P.A. Thiessen, et al., Per- and Polyfluoroalkyl Substances (PFAS) in PubChem: 7 Million and Growing, Env. Sci. Technol. 57 (2023) 16918–16928, https://doi.org/10.1021/acs.est.3c04855.
[5] K.E. Pelch, A. Reade, T.A.M. Wolffe, et al., PFAS health effects database: protocol for a systematic evidence map, Env. Int. 130 (2019) 104851, https://doi.org/10.1016/j.envint.2019.05.045.
[6] D. Renfrew, T.W. Pearson, The Social Life of the "Forever Chemical": PFAS Pollution Legacies and Toxic Events, Env. Soc. 12 (2021) 146–163, https://doi.org/10.3167/ares.2021.120109.
[7] J.C. DeWitt, Toxicological Effects of Perfluoroalkyl and Polyfluoroalkyl Substances - National Library of Medicine Institution, Springer International Publishing, Basel, 2015.
[8] J.L. Domingo, M. Nadal, Human exposure to per- and polyfluoroalkyl substances (PFAS) through drinking water: a review of the recent scientific literature, Env. Res. 177 (2019) 108648, https://doi.org/10.1016/j.envres.2019.108648.
[9] A. Ramírez Carnero, A. Lestido-Cardama, P. Vazquez Loureiro, et al., Presence of perfluoroalkyl and polyfluoroalkyl substances (PFAS) in food contact materials (FCM) and its migration to Food, Foods 10 (2021) 1443, https://doi.org/10.3390/foods10071443.
[10] EU, Directive (EU) 2020/2184 of the European Parliament and of the Council of 16 December 2020 on the quality of water intended for human consumption 2020, accessed, https://eur-lex.europa.eu/eli/dir/2020/2184/oj/eng, June 8, 2026. accessed.
[11] T. Teymoorian, G. Munoz, S. Sauvé, PFAS contamination in tap water: target and suspect screening of zwitterionic, cationic, and anionic species across Canada and beyond, Env. Int. 195 (2025) 109250, https://doi.org/10.1016/j.envint.2025.109250.
[12] M.D. Al Amin, Z. Sobhani, Y. Liu, et al., Recent advances in the analysis of per- and polyfluoroalkyl substances (PFAS)—A review, Env. Techn. Innov. 19 (2020) 100879, https://doi.org/10.1016/j.eti.2020.100879.
[13] D. Grgas, A. Petrina, T. Štefanac, et al., A review: per- and polyfluoroalkyl substances—biological degradation, Toxics 11 (2023) 446, https://doi.org/10.3390/toxics11050446.
[14] Z. Wang, I.T. Cousins, M. Scheringer, et al., Global emission inventories for C4–C14 perfluoroalkyl carboxylic acid (PFCA) homologues from 1951 to 2030, Part I: production and emissions from quantifiable sources, Env. Int. 70 (2014) 62–75, https://doi.org/10.1016/j.envint.2014.04.013.
[15] Y. Zhi, X. Lu, G. Munoz, et al., Environmental occurrence and biotic concentrations of ultrashort-chain perfluoroalkyl acids: overlooked global organofluorine contaminants, Env. Sci. Technol. 58 (2024) 21393–21410, https://doi.org/10.1021/acs.est.4c04453.
[16] I.S. Gkika, J. Arie Vonk, T.L. ter Laak, et al., Strong bioaccumulation of a wide variety of PFAS in a contaminated terrestrial and aquatic ecosystem, Env. Int. 202 (2025) 109629, https://doi.org/10.1016/j.envint.2025.109629.
[17] M.K. Björnsdotter, L.W.Y. Yeung, A. Kärrman, et al., Challenges in the analytical determination of ultra-short-chain perfluoroalkyl acids and implications for environmental and human health, Anal. Bioanal. Chem. 412 (2020) 4785–4796, https://doi.org/10.1007/s00216-020-02692-8.
[18] European Chemicals Agency (ECHA), CLH report: sodium trifluoroacetate – Proposal for harmonised classification and labelling, Document No. 47154. ECHA 2025, accessed, https://echa.europa.eu/documents/10162/2842450/clh_rcom_sodium+trifluoroacetate_47154_en.pdf, July 30, 2026. accessed.
[19] H.P.H. Arp, A. Gredelj, J. Glüge, et al., The Global Threat from the Irreversible Accumulation of Trifluoroacetic Acid (TFA), Env. Sci. Technol. 58 (2024) 19925–19935, https://doi.org/10.1021/acs.est.4c06189.
[20] A.L.B. Forster, Y. Zhang, D.C. Westerman, et al., Improved total organic fluorine methods for more comprehensive measurement of PFAS in industrial wastewater, river water, and air, Water Res. 235 (2023) 119859, https://doi.org/10.1016/j.watres.2023.119859.
[21] F. Dixit, E.H. Antell, K.A. Faber, et al., Closing PFAS analytical gaps: inter-method evaluation of total organofluorine techniques for AFFF-impacted water, J. Hazard. Mater. Lett. 5 (2024) 100122, https://doi.org/10.1016/j.hazl.2024.100122.
[22] A. Androulakakis, N. Alygizakis, E. Bizani, et al., Current progress in the environmental analysis of poly- and perfluoroalkyl substances (PFAS), Env. Sci. Adv. 1 (2022) 705–724, https://doi.org/10.1039/D2VA00147K.

[23] M. Stróżyńska, K. Schuhen, Extraction and derivatization for perfluorocarboxylic acids in liquid and solid matrices: a review, Anal Sci. Adv. 2 (2021) 343–353, https://doi.org/10.1002/ansa.202000089.
[24] J. Freilinger, J.O. Back, R. Plangger, et al., Development of a fluorophilic ion-exchange material with dual binding mechanism for solid-phase extraction of PFAS, J. Hazard. Mater. Lett. 6 (2025) 100158, https://doi.org/10.1016/j.hazl.2025.100158.
[25] M. Brumovský, J. Bečanová, P. Karásková, et al., Retention performance of three widely used SPE sorbents for the extraction of perfluoroalkyl substances from seawater, Chemosphere 193 (2018) 259–269, https://doi.org/10.1016/j.chemosphere.2017.10.174.
[26] P. Jacob, D.E. Helbling, Rapid and Simultaneous Quantification of Short- and Ultrashort-Chain Perfluoroalkyl Substances in Water and Wastewater, ACS EST Water 3 (2023) 118–128, https://doi.org/10.1021/acsestwater.2c00446.
[27] J. Janda, K. Nödler, H.-J. Brauch, et al., Robust trace analysis of polar (C2-C8) perfluorinated carboxylic acids by liquid chromatography-tandem mass spectrometry: method development and application to surface water, groundwater and drinking water, Env. Sci. Pollut. Res. 26 (2019) 7326–7336, https://doi.org/10.1007/s11356-018-1731-x.
[28] R. Ye, R.A. Di Lorenzo, J.T. Clouthier, et al., A rapid derivatization for quantitation of perfluorinated carboxylic acids from aqueous matrices by gas chromatography–mass spectrometry, Anal. Chem. 95 (2023) 7648–7655, https://doi.org/10.1021/acs.analchem.3c00593.
[29] A. Aw, M. Fritz, J.W. Napoline, et al., Continuous Flow Chemistry: reaction of Diphenyldiazomethane with p-Nitrobenzoic Acid, J. Vis. Exp. (2017) 56608, https://doi.org/10.3791/56608.
[30] A.L. Rockwood, M.M. Kushnir, N.J. Clarke, Mass Spectrometry. Principles and Applications of Clinical Mass Spectrometry,, Elsevier, 2018, pp. 33–65, https://doi.org/10.1016/B978-0-12-816063-3.00002-5.
[31] ICH Q2(R2), Validation of analytical procedures - scientific guideline | european medicines agency (EMA), 2024 Step - Revision 2 n.d, accessed, https://www.ema.europa.eu/en/ich-q2r2-validation-analytical-procedures-scientific-guideline, June 8, 2026. accessed.
[32] S. Henne, F.R. Storck, H. Wöhrnschimmel, et al., Trifluoroacetate (TFA) in precipitation and surface waters in Switzerland: trends, source attribution, and budget, Atmos. Chem. Phys. 25 (2025) 18157–18186, https://doi.org/10.5194/acp-25-18157-2025.
[33] T.D. Saliu, T. Teymoorian, G. Munoz, et al., Analysis of ultra-short-chain and short-chain PFAS in environmental samples: a review, Talanta 306 (2026) 129745, https://doi.org/10.1016/j.talanta.2026.129745.
[34] R. Sayed, A.A. Omran, R.S. Farag, et al., Overcoming challenges in the analysis of the ubiquitous emerging contaminant trifluoroacetic acid employing trap column liquid chromatography tandem mass spectrometry, J. Hazard. Mater. 491 (2025) 137976, https://doi.org/10.1016/j.jhazmat.2025.137976.
[35] Q. Fan, L. Guo, G. Wu, et al., Ce3+-doped Cs3Bi2Br9 for photocatalytic selective oxidation of alcohols to aldehydes/ketones, Inorg. Chem. 65 (2026) 1852–1862, https://doi.org/10.1021/acs.inorgchem.5c04499.
[36] D. Zehavi, J.N. Seiber, An analytical method for trifluoroacetic acid in water and air samples using headspace gas chromatographic determination of the methyl ester, Anal. Chem. 68 (1996) 3450–3459, https://doi.org/10.1021/ac960128s.
[37] M. Stróżyńska, K. Schuhen, Dispersive solid-phase extraction followed by triethylsilyl derivatization and gas chromatography mass spectrometry for perfluorocarboxylic acids determination in water samples, J. Chromatogr. A 1597 (2019) 1–8, https://doi.org/10.1016/j.chroma.2019.03.008.